2025 IEEE International Conference on Robotics and Automation (ICRA 2025)
May 19-23, 2025. Atlanta, USA

Intelligent Self-Healing Artificial Muscle: Mechanisms for Damage Detection and Autonomous Repair of Puncture Damage in Soft Robotics

Ethan J. Krings*, Patrick McManigal*, and Eric J. Markvicka

Abstract— **Soft robotics are characterized by their high deformability, mechanical robustness, and inherent resistance to damage. These unique properties present exciting new opportunities to enhance both emerging and existing fields such as healthcare, manufacturing, and exploration. However, to function effectively in unstructured environments, these technologies must withstand the same real-world conditions to which human skin and other soft biological materials are typically subjected. Here, we present a novel soft material architecture designed for active detection of material damage and autonomous repair in soft robotic actuators. By integrating liquid metal (LM) microdroplets within a silicone elastomer, the system can detect and localize damage through the formation of conductive pathways that arise from extreme pressure ($>$ 1 MPa) or puncture events. These newly formed conductive networks function as in situ Joule heating elements, facilitating the reprocessing and healing of the material. The architecture allows for the reconfiguration of the newly formed electrical network using controlled electrical and thermal mechanisms to restore functionality. The entire process from damage detection to repair and reconfiguration occurs without any manual intervention or external mechanisms to facilitate healing. This innovative approach not only enhances the resilience and performance of soft materials but also supports a wide range of applications in soft robotics and wearable technologies, where adaptive and autonomous systems are crucial for operation in dynamic and unpredictable environments.**

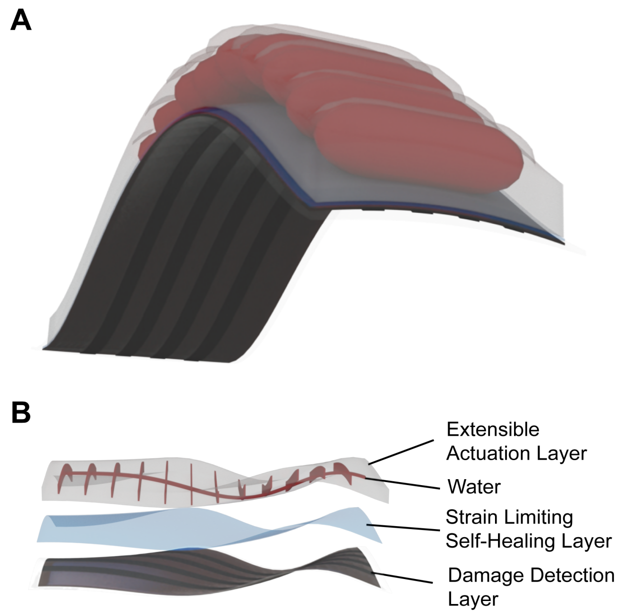

Fig. 1. A) Schematic illustration of the intelligent self-healing artificial muscle. B) Exploded schematic illustration of the layered architecture and integration of advanced materials to enable the artificial muscle to sense damage and facilitate self-repair mechanisms without manual intervention or external healing mechanisms.

I. Introduction

Soft materials with sensing, actuation, and self-healing capabilities are enabling a new generation of multifunctional technologies for applications ranging from bio-inspired soft robotics to wearable computing. These materials are highly deformable, mechanically robust, and naturally damage resistant and can withstand compressive forces, impacts, and bending that would typically damage rigid counterparts of similar size and weight [1], [2], [3], [4]. However, as soft-matter technologies transition from controlled laboratories to real-world environments, they must be able to endure the same conditions faced by human skin and other soft biological materials. To achieve this, these materials must have the ability to detect and respond to external stimuli, communicate damage information, and include self-healing mechanisms – mimicking the remarkable adaptive resilience of living organisms. Incorporating these biomimetic functionalities is essential for ensuring the longevity of soft robotic and wearable systems as they interact with unpredictable real-world environments.

Ethan J. Krings, Patrick McManigal, and E. J. Markvicka are with the Smart Materials and Robotics Laboratory, Department of Mechanical & Materials Engineering, University of Nebraska-Lincoln, Lincoln, NE 68588, USA (*Ethan J. Krings and Patrick McManigal are co-first authors.) (Corresponding author: Eric Markvicka eric.markvicka@unl.edu)

Human nervous tissue serves as an exemplary model of a soft, responsive material capable of detecting, communicating, and recovering from injuries through its inherent plasticity. This characteristic is particularly relevant for soft robotics designed for agricultural applications, which are often exposed to sharp objects such as twigs, thorns, plastic, or glass that can cause damage to these systems [5]. To address this vulnerability, numerous studies have explored self-healing polymeric and elastomeric materials for soft robotics applications that employ a variety of mechanisms to achieve self-repair [6], [7], [8], [9], [10], [11], [12], [13], [14], [15], [16]. These advancements have led to the development of soft systems with self-healing capabilities in sensors [17], [18], [12], electrical wiring [19], [20], [21], and actuation [22], [23], [24], [15]. A promising strategy for autonomous self-healing is based on the integration of Joule heating elements with self-healing polymers [15], [13], [25]. This approach eliminates the need for manual intervention or external stimuli, representing a significant step towards robust, autonomous soft robotic systems. Despite these promising developments, the comprehensive integration of damage detection, communication, and recovery in soft-robotic technologies remains a significant challenge [1].

Here, we introduce a novel soft material architecture for active detection of material damage and autonomous repair through in situ reprocessing and reconfiguration of both the material structure and its electrical network (Fig. 1). This architecture includes a soft electronic skin composed of LM microdroplets embedded within a silicone elastomer, enabling the detection and localization of damage by monitoring the formation of conductive pathways resulting from extreme pressure ($>$ 1 MPa) or puncture events [18]. The newly created conductive networks serve as in situ Joule heating elements to facilitate the reprocessing and healing of physically cross-linked polymer layers. Following the self-healing process, these electrical networks can be reconfigured using electromigration and thermal mechanisms to create physical discontinuities. This system level integration enables electrical damage detection and localization, self-healing capabilities for extreme damage events, and the reconfiguration of newly formed electrical networks–all without the need for manual intervention or external mechanisms. This approach not only enhances the resilience and functionality of soft materials, but also paves the way for advanced applications in soft robotics and wearable technologies, where adaptive and autonomous systems are essential for continuous operation in dynamic and unstructured environments.

II. Soft Electronic Skin

A. Manufacturing

The soft electronic skin utilizes an LM elastomer composite material architecture. This material was created by shear mixing Ga-based LM (75% gallium, 25% indium by weight, Rotometals) with uncured silicone elastomer (Sylgard 184, Dow) at a 1:1 volume ratio, forming a suspension of LM microdroplets ($\sim$100 μm particles). A layer of silicone elastomer is first applied to a glass substrate and cured. A mask is then applied, and a layer of the LM-composite is cast and cured. A final layer of elastomer is then cast on top of the LM-composite and subsequently cured. All layers are 0.5 mm thick, applied using a thin film applicator, and cured at 100 °C for 1 hour. Previous research by the authors and others has demonstrated the versatility of LM elastomer composites in terms of material properties. These composites can be engineered to exhibit extreme toughness [26], exceptional electrical and thermal characteristics [27], [28], [29], [30], [31], [32], [33], [34], [35], [36], [37], and the ability to form electrically conductive pathways [19], [18], [38], [39], [40], [41], [42].

B. Formation of Electrical Networks

Following synthesis, the LM composite is electrically insulating. The application of extreme pressure ($>$ 1 MPa) or puncture events induces the formation of conductive traces that are internal to the composite and can function as traces for power or signal transmission [19]. The remaining material surrounding these traces remains unaffected and allows multiple electrically insulating traces to be formed within a single composite. To ensure consistent results across samples, the conductive traces were created using an X-Y pen plotter (Maker 3, Cricut) equipped with a scoring wheel to selectively apply pressure to predefined regions. Trace width was controlled by adjusting the number of adjacent line paths and the depth of the traces was controlled by adjusting the thickness of the LM elastomer composite.

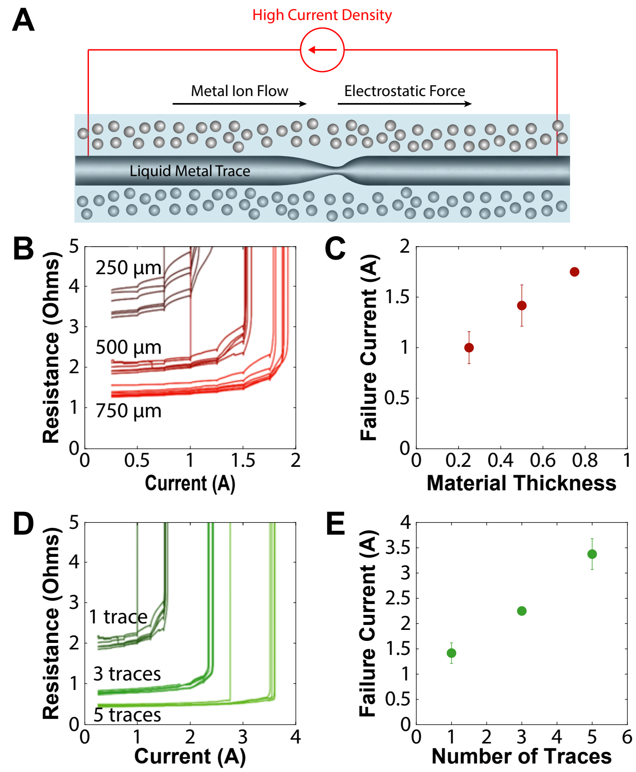

Fig. 2. Electrical network behavior as a function of applied current. A) Schematic illustration of controlled electromigration and thermal failure mechanisms. Failure occurs due to metal ion flow at high current density and thermal expansion mismatch between the two materials. B) Resistance as a function of applied current. C) Failure current presented as mean $\pm$ s.d. ($n = 6$) for LM composite thicknesses of 250, 500, and 750 μm. D) Resistance as a function of applied current. E) Failure current presented as mean $\pm$ s.d. ($n = 6$) for trace widths of 1, 3, and 5 traces.

C. Reconfiguration of Electrical Networks

The electrical networks created in LM elastomer composites are generally considered permanent, especially in conventional thermosets with covalent networks. Physically cross-linked polymers, such as themoplastic elastomers, can be reprocessed with manual intervention through the use of solvents or heating to reconfigure the polymer and electrical networks [20], [21]. In this study, we demonstrate that electrical networks created in thermoset elastomers can be reconfigured using controlled electrical processes without modifying the elastomer network (Fig. 2A). Physical discontinuities in the electrical networks are created at high current densities, where electromigration and thermal failure mechanisms are observed [43], [44], [45], [46], [47], [48], [49].

To systematically investigate the impact of trace cross sectional area on electromigration and thermal failure mechanisms, we varied the width and thickness of the conductive traces. The trace width was controlled by creating multiple adjacent line paths, while the depth of the trace was adjusted

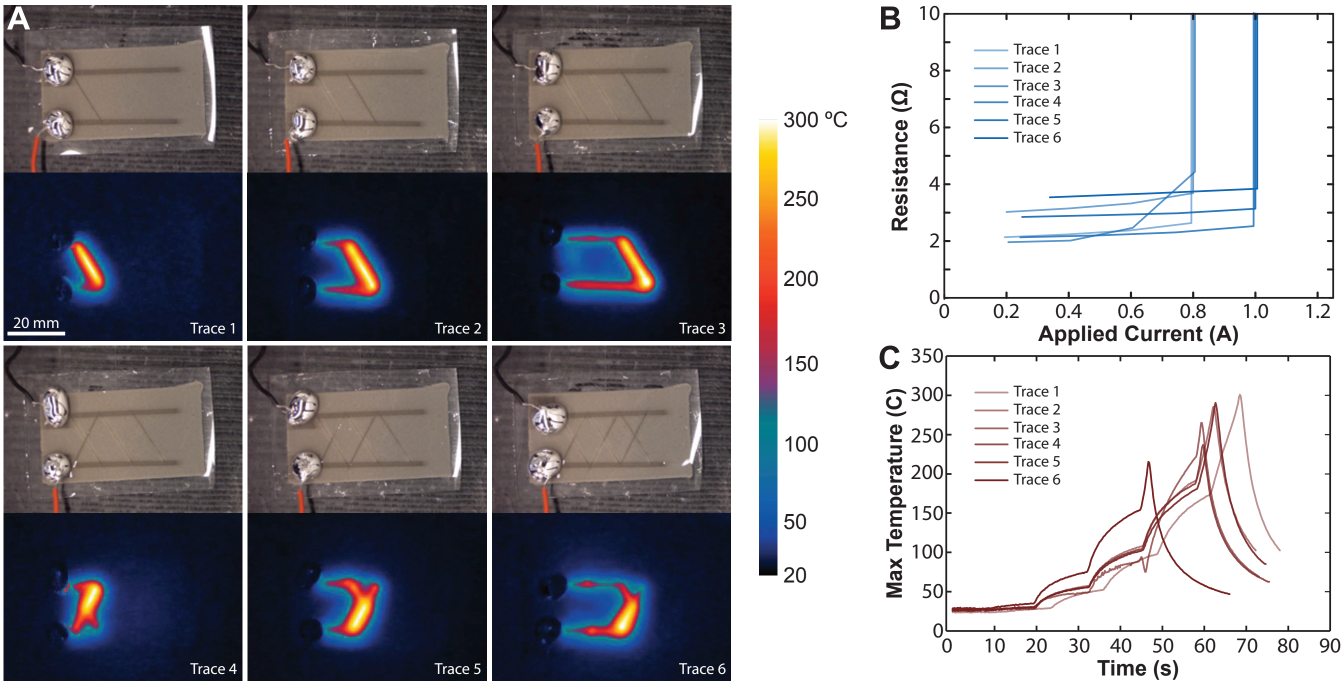

Fig. 3. Reconfiguration of significant pressure damage. A) (Top) Photographs of the soft electronic skin showing pressure damage (> 1 MPa). (Bottom) Thermal camera snapshots captured just before electromigration and thermal failure, which triggered the reconfiguration of the electrical network. The process was repeated six times to assess consistency and reliability. B) Sample resistance as a function of applied current during the reconfiguration process. C) Maximum sample temperature over time as a ramping current was applied in increments 0.25 amps every 10 seconds, until the electrical trace was reconfigured and electrical conductivity was lost due to open circuit failure.

by modifying the thickness of the LM elastomer composite. LM electrodes were deposited at the end of each trace and connected to a programmable DC power supply (2260, Keithley). A ramping current was applied in increments of 0.25 amps every 30 seconds until the electrical trace was reconfigured and electrical conductivity was lost due to open circuit failure. Notably, the visual appearance of the trace changed from dark gray to a lighter, cloudy gray after failure with no observable changes to surface roughness. As shown in Fig. 2B and D, the resistance of the trace gradually increased until a significant change occurred, resulting in the loss of electrical conductivity. The current required for circuit reconfiguration was found to increase as the thickness of the LM composite increased from 250 μm to 750 μm (Fig. 2C) and as the trace width increased from one to five adjacent traces (Fig. 2E). The most substantial change in current, ranging from 1.5 to 3.5 amps, correlated with the increase in trace width from one to five traces. This ability to tailor the patterned trace area provides new opportunities to control the specific location where circuit reconfiguration occurs in LM elastomer composites.

III. Electrical Detection and Reconfiguration of Damage Events

Local damage between two adjacent conductive traces can be detected by monitoring their impedance. When damage occurs in an area that overlaps both traces, new electrical pathways are formed around the damaged region, thereby lowering their impedance and electrically connecting the two traces. This newly formed electrical pathway can then be reconfigured through electromigration and thermal failure mechanisms. Electromigration and thermal failure occurs in the area of highest impedance. If the expected size of damage is known, the patterned traces can be designed sufficiently large to ensure the circuit is reconfigured within the damaged area.

To demonstrate that damage can be electrically detected and subsequently reconfigured, we drew two 2 mm wide monitoring traces (each consisting of five adjacent lines per trace) with a center-to-center spacing of 17 mm. Electrodes were patterned on one end of each trace to serve as an electrical interface and were connected to a programmable DC power supply. Various damage types, such as pressure and cutting, were then applied between the two monitoring traces to form a conductive pathway between the traces. This pathway was detected by applying a small voltage (1 volt) and measuring current to determine if the electrical circuit was complete. Once continuity was established, a ramping current was applied in increments of 0.25 amps every 10 seconds in constant current mode until electromigration and thermal failure occurred, which electrically reconfigured the circuit and caused an open circuit failure in the damaged region. This process was repeated until a total of six damage and reconfiguration cycles were completed for each damage type per sample. This systematic approach allowed for the reliable evaluation of the electronic skin's performance under various damage scenarios and reconfiguration cycles.

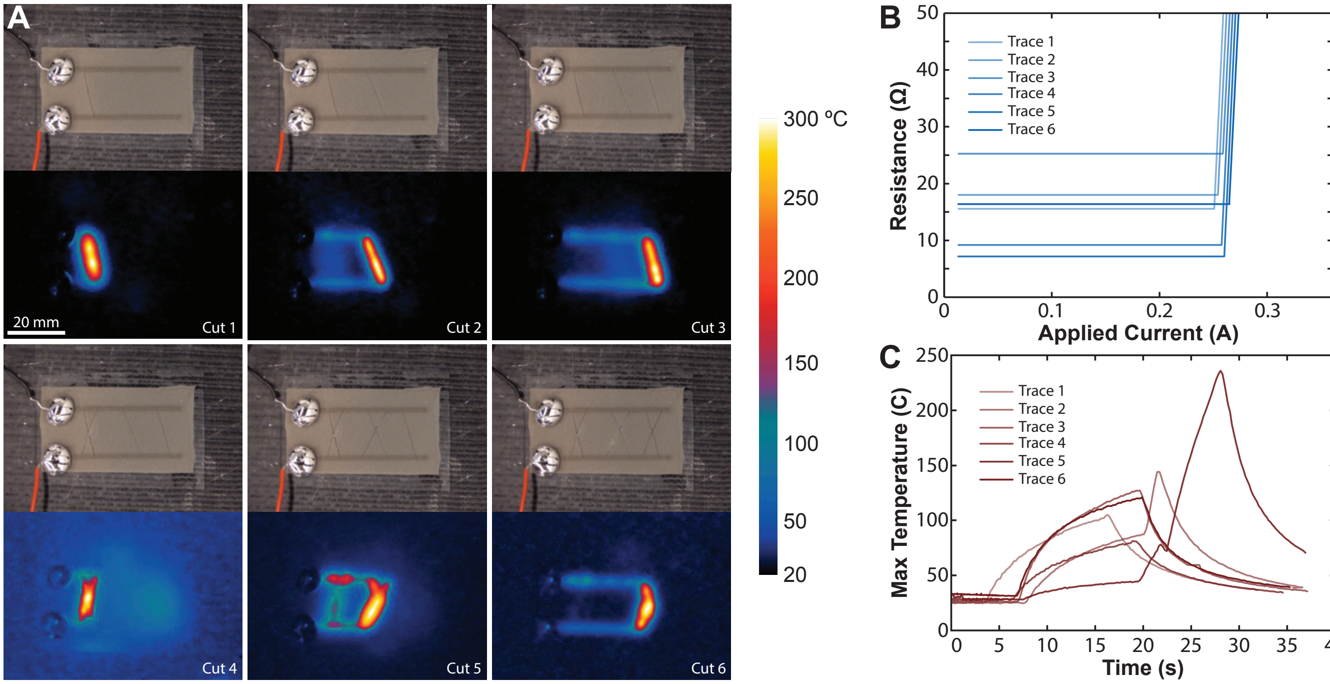

Fig. 4. Reconfiguration of puncture damage. A) (Top) Photographs of the soft electronic skin showing puncture damage. (Bottom) Thermal camera snapshots captured just before electromigration and thermal failure, which triggered the reconfiguration of the electrical network. The process was repeated six times to assess consistency and reliability. B) Sample resistance as a function of applied current during the reconfiguration process. C) Maximum sample temperature over time as a ramping current was applied in increments 0.25 amps every 10 seconds, until the electrical trace was reconfigured and electrical conductivity was lost due to open circuit failure.

A. *Pressure Damage*

Significant pressure damage was applied to the sample using the scoring wheel attachment on the X-Y plotter, resulting in a single trace electrically connecting the two adjacent monitoring traces, which consist of five traces each (Fig. 3A, Trace 1). After continuity was established, a current ramp was applied until an open circuit failure occurred, during which the sample's resistance and temperature were measured. As shown in Fig. 3B, the resistance of the trace gradually increased until a threshold was reached, leading to the loss of electrical conductivity and simultaneous reconfiguration of the electrical network. The location of electromigration and thermal failure is confirmed using a thermal camera, with frames shown in Fig 3A captured just before failure occurred. The hottest area directly corresponds to the damaged area and location of electromigration and thermal failure. Prior to electromigration and thermal failure, the material experiences elevated temperatures exceeding 200 °C at the damage location (Fig. 3C). Silicone elastomers exhibit exceptional thermal stability at elevated temperatures, remaining stable up to 300 °C under vacuum [50].

B. *Puncture Damage*

Puncture damage was applied to the sample using a precision knife, which cut through both monitoring traces (Fig. 4A). After continuity was established, a current ramp was applied until an open circuit failure occurred, during which the sample's resistance and temperature were measured. As shown in Fig. 4B, the resistance of the trace gradually increased until a threshold was reached, leading to the loss of electrical conductivity and the simultaneous reconfiguration of the electrical network. The area of damage, represented by a single cut, is smaller and involves a different mechanism of network formation compared to the monitoring traces, which consist of five traces formed through pressure application. The location of electromigration and thermal failure was confirmed using a thermal camera, with frames shown in Fig. 3A captured just before failure occurred. Prior to electromigration and thermal failure, the material experienced elevated temperatures exceeding 100 °C at the damage site (Fig. 3C). Puncture damage is a common concern in soft robotics, particularly when these soft systems encounter sharp objects or rough surfaces during operation. Addressing this vulnerability through effective detection and self-healing mechanisms is crucial for ensuring the reliability and longevity of soft robotic systems, as pressure or fluid leakage resulting from puncture can lead to reduced performance and unexpected failures.

IV. Soft Robotics Application

A self-healing artificial muscle is created with embedded sensors to allow the system to continuously monitor for damage, such as puncture damage, in real-time (Fig. 5). Upon detecting damage, the actuator can initiate an autonomous repair process through in situ reprocessing, where Joule heating is used to trigger a self-healing material layer. Following self-healing, the damaged area is reconfigured, restoring functionality without the need for manual intervention or external healing mechanisms. The integration of these features not only enhances the resilience of the soft robotic

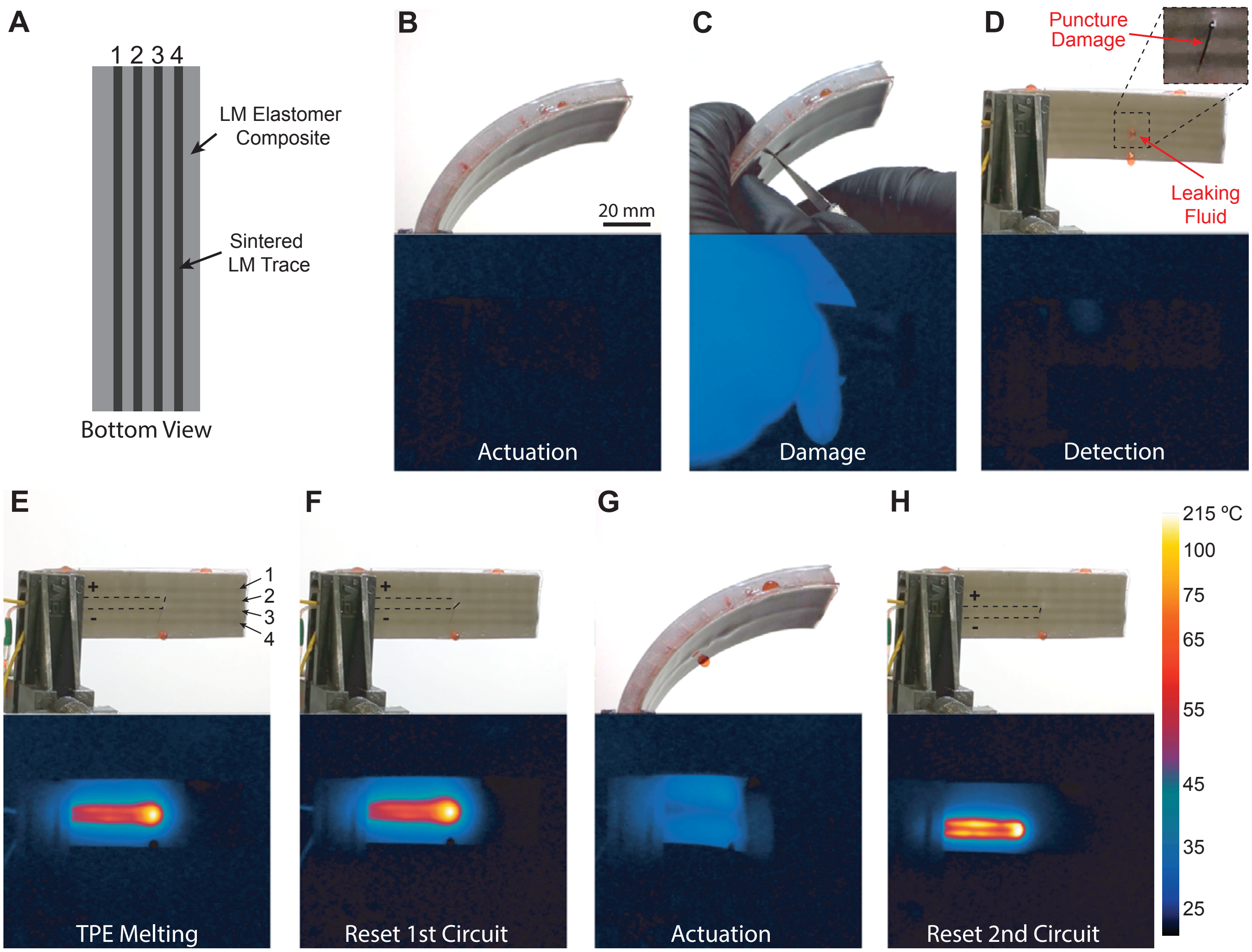

Fig. 5. Intelligent self-healing artificial muscle. A) Bottom view of the actuator and configuration of the damage detection layer with four traces to detect damage events. B) The actuator was pressurized with dyed water and C) punctured with a precision knife. D) This damage event caused damage to both the damage detection layer (between traces 2, 3, and 4) and self-healing TPE layer. Fluid is shown leaking from the actuator. E) The actuator was depressurized and a current was applied between traces 2 and 3 to melt the self-healing TPE layer and seal the puncture. F) The current was then increased, causing electromigration and thermal failure to reconfigure the electrical network. G) The actuator was pressurized again and functioned as expected. H) The damage detection layer was fully reset by applying a current ramp between trace 3 and 4 until electromigration and thermal failure occurred reconfiguring the electrical network.

actuator but also mimics the adaptive capabilities found in biological systems, ultimately leading to more reliable and efficient performance in dynamic environments.

A. Design

A soft robotic actuator was designed consisting of a silicone elastomer layer with a series of bladders that was bonded to a stiffer, inextensible thermoplastic elastomer (TPE) layer (Fig. 1). The soft electronic skin consisting of a LM elastomer composite was then adhered to the TPE layer. When the top silicone layer was inflated with water, the difference in strain between the extensible top layer and inextensible bottom layers causes the actuator to bend. The soft electronic skin contained four parallel traces that were used to detect the location of damage by monitoring the impedance between each trace (Fig. 5A). If continuity was detected, the newly formed electrical network has a high resistance relative to the four monitoring traces, allowing the newly formed electrical network to function as a local Joule heater. The Joule heating element can be used to locally heat the punctured area for several minutes to melt the TPE layer and self-heal the puncture damage, allowing the actuator to continue to operate as before. After self-healing, the circuit can be reconfigured by increasing the applied current until electromigration and thermal failure occurs, resulting in an open circuit failure. This resets the damage detection network, allowing a new damage event to be detected, self-healed, and reconfigured. As previously noted, silicone elastomers have exceptional thermal stability and are not degraded at the elevated temperatures required for healing or reconfiguration.

B. Manufacturing

The series of inflatable bladders was fabricated by mixing and degassing a silicone elastomer (ExSil 100, Gelest) at a ratio of 100:1 prepolymer to crosslinker. The uncured elastomer was then cast into a PTFE mold and cured at 100 °C for 8 hours. A Styrene-ethylene-butylene-styrene (SEBS) TPE (H1521, Asahi Kasei) was dissolved in toluene at a ratio of 25 g SEBS to 70 ml solvent. The dissolved SEBS was degassed for 10 minutes before being cast onto a glass sheet and left under a fume hood overnight to allow the toluene to evaporate. The LM elastomer damage detection layer was fabricated as described above in Section II. To bond the layers, both were treated with oxygen plasma, while one layer was submerged in an aqueous solution of 4% v/v APTES (440140, Sigma Aldrich) for 15 minutes and then dried with compressed air [51], [52]. The layers were assembled and placed in an oven at 80 °C for 15 minutes. Although the presented demonstration is predominately flat, other geometries, such as cylindrical shapes, could be achieved using injection or compression molding techniques.

C. Validation of Self-Healing Actuator

The self-healing soft robotic actuator was pressurized with dyed water and punctured using a precision knife while under pressure (Fig. 5B, C). This puncture event damaged both the damage detection layer and self-healing TPE layer, causing the red fluid to leak out of the actuator and electrically connect traces 2, 3, and 4 (Fig. 5D). After depressurizing the actuator, a current of 0.5 amps was applied between traces 2 and 3 to locally increase the temperature, melt the self-healing TPE layer, and seal the puncture (Fig. 5E, F). As shown in the thermal images, the surface temperature of the LM elastomer composite reached over 210 °C (Fig. 5). After approximately 2 minutes, the current was increased until electromigration and thermal failure occurred, reconfiguring the electrical network. The actuator was then pressurized again, and no water leaked from the puncture location, indicating the actuator was successfully healed without manual intervention or external healing mechanisms. To fully reset the damage detection layer, a current ramp was applied to the second circuit (between traces 3 and 4) until electromigration and thermal failure occurred, effectively reconfiguring the damage detection layer to its initial state. There was no visible changes to the surface of the actuator after the healing and reconfiguration cycles.

This demonstration highlights the self-healing capabilities of the soft robotic actuator, which can autonomously detect and repair damage to restore functionality without requiring manual intervention or external mechanisms. This innovative approach improves the resilience and performance of soft robotic actuators, enabling their widespread adoption in various applications, particularly in dynamic and unpredictable environments. Nonetheless, additional experimentation is required to fully understand the limitations of the system, such as the maximum number of damage and healing cycles that can be sustained by the self-healing actuator [23].

V. Conclusions

In summary, we have introduced a self-healing artificial muscle capable of detecting material damage and facilitating self-repair autonomously, without the need for manual intervention or external healing mechanisms. Damage events, such as extreme pressure or punctures, are detected and localized by monitoring the formation of new electrical networks between existing traces. These newly formed electrical networks created by damage events enable localized Joule heating to activate the self-healing material layer. The Joule heating element is used to locally heat the punctured area, melt the self-healing TPE layer, and seal the damaged area. By continuing to increase the applied current, the newly formed electrical network can be reconfigured using controlled electrical and thermal mechanisms to create physical discontinuities and restore the functionality of the damage detection layer. This system-level integration of active damage detection and autonomous self-repair can be seamlessly incorporated into a wide range of soft, flexible, or rigid materials without increasing mechanical stiffness. As a result, this technology can support various emerging applications, from bio-inspired soft robotics to wearable computing. This is especially relevant for soft robotics designed for agricultural applications, which are often exposed to sharp objects such as twigs, thorns, plastic, or glass that can cause damage to these systems.

Acknowledgment

The authors acknowledge support through the National Science Foundation (No. CMMI-2339780), NASA Nebraska EPSCoR (80NSSC19M0065), and the Nebraska Tobacco Settlement Biomedical Research Development Fund. We acknowledge K. Moomau for support with electromigration and thermal failure experiments.

References

[1] R. A. Bilodeau and R. K. Kramer, "Self-healing and damage resilience for soft robotics: A review," *Frontiers in Robotics and AI*, vol. 4, p. 48, 2017.

[2] R. V. Martinez, A. C. Glavan, C. Keplinger, A. I. Oyetibo, and G. M. Whitesides, "Soft actuators and robots that are resistant to mechanical damage," *Advanced Functional Materials*, vol. 24, no. 20, pp. 3003–3010, 2014.

[3] M. T. Tolley, R. F. Shepherd, B. Mosadegh, K. C. Galloway, M. Wehner, M. Karpelson, R. J. Wood, and G. M. Whitesides, "A resilient, untethered soft robot," *Soft robotics*, vol. 1, no. 3, pp. 213–223, 2014.

[4] Y. J. Tan, G. J. Susanto, H. P. Anwar Ali, and B. C. Tee, "Progress and roadmap for intelligent self-healing materials in autonomous robotics," *Advanced Materials*, vol. 33, no. 19, p. 2002800, 2021.

[5] J. Shintake, V. Cacucciolo, D. Floreano, and H. Shea, "Soft robotic grippers," *Advanced materials*, vol. 30, no. 29, p. 1707035, 2018.

[6] T.-P. Huynh, P. Sonar, and H. Haick, "Advanced materials for use in soft self-healing devices," *Advanced Materials*, vol. 29, no. 19, p. 1604973, 2017.

[7] N. Zheng, Y. Xu, Q. Zhao, and T. Xie, "Dynamic covalent polymer networks: a molecular platform for designing functions beyond chemical recycling and self-healing," *Chemical Reviews*, vol. 121, no. 3, pp. 1716–1745, 2021.

[8] B. Li, P.-F. Cao, T. Saito, and A. P. Sokolov, "Intrinsically self-healing polymers: from mechanistic insight to current challenges," *Chemical Reviews*, vol. 123, no. 2, pp. 701–735, 2022.

[9] R. P. Wool, "Self-healing materials: a review," *Soft Matter*, vol. 4, no. 3, pp. 400–418, 2008.

[10] D. Y. Wu, S. Meure, and D. Solomon, "Self-healing polymeric materials: A review of recent developments," *Progress in polymer science*, vol. 33, no. 5, pp. 479–522, 2008.

[11] S. Terryn, J. Langenbach, E. Roels, J. Brancart, C. Bakkali-Hassani, Q.-A. Poutrel, A. Georgopoulou, T. G. Thuruthel, A. Safaei, P. Ferrentino, *et al.*, "A review on self-healing polymers for soft robotics," *Materials Today*, vol. 47, pp. 187–205, 2021.

[12] M. Khatib, O. Zohar, W. Saliba, and H. Haick, "A multifunctional electronic skin empowered with damage mapping and autonomic acceleration of self-healing in designated locations," *Advanced Materials*, vol. 32, no. 17, p. 2000246, 2020.

[13] S. K. Tabrizian, F. Sahraeeazartamar, J. Brancart, E. Roels, P. Ferrentino, J. Legrand, G. Van Assche, B. Vanderborght, and S. Terryn, "A healable resistive heater as a stimuli-providing system in self-healing soft robots," *IEEE Robotics and Automation Letters*, vol. 7, no. 2, pp. 4574–4581, 2022.

[14] W. Tang, Y. Zhong, H. Xu, K. Qin, X. Guo, Y. Hu, P. Zhu, Y. Qu, D. Yan, Z. Li, *et al.*, "Self-protection soft fluidic robots with rapid large-area self-healing capabilities," *Nature Communications*, vol. 14, no. 1, p. 6430, 2023.

[15] S. Kashef Tabrizian, S. Terryn, A. C. Cornellà, J. Brancart, J. Legrand, G. Van Assche, and B. Vanderborght, "Assisted damage closure and healing in soft robots by shape memory alloy wires," *Scientific Reports*, vol. 13, no. 1, p. 8820, 2023.

[16] S. Kashef Tabrizian, S. Terryn, and B. Vanderborght, "Toward autonomous self-healing in soft robotics: A review and perspective for future research," *Advanced Intelligent Systems*, p. 2400790.

[17] W. W. Lee, Y. J. Tan, H. Yao, S. Li, H. H. See, M. Hon, K. A. Ng, B. Xiong, J. S. Ho, and B. C. Tee, "A neuro-inspired artificial peripheral nervous system for scalable electronic skins," *Science Robotics*, vol. 4, no. 32, p. eaax2198, 2019.

[18] E. J. Markvicka, R. Tutika, M. D. Bartlett, and C. Majidi, "Soft electronic skin for multi-site damage detection and localization," *Advanced Functional Materials*, vol. 29, no. 29, p. 1900160, 2019.

[19] E. J. Markvicka, M. D. Bartlett, X. Huang, and C. Majidi, "An autonomously electrically self-healing liquid metal–elastomer composite for robust soft-matter robotics and electronics," *Nature materials*, vol. 17, no. 7, pp. 618–624, 2018.

[20] R. Tutika, A. T. Haque, and M. D. Bartlett, "Self-healing liquid metal composite for reconfigurable and recyclable soft electronics," *Communications Materials*, vol. 2, no. 1, p. 64, 2021.

[21] M. J. Ford, D. K. Patel, C. Pan, S. Bergbreiter, and C. Majidi, "Controlled assembly of liquid metal inclusions as a general approach for multifunctional composites," *Advanced Materials*, vol. 32, no. 46, p. 2002929, 2020.

[22] S. Terryn, J. Brancart, D. Lefeber, G. Van Assche, and B. Vanderborght, "Self-healing soft pneumatic robots," *Science Robotics*, vol. 2, no. 9, p. eaan4268, 2017.

[23] J. Legrand, A. Abdulali, D. Hardman, S. Terryn, B. Vanderborght, and F. Iida, "Autonomous testing of the repeatable healability of pneumatic self-healing soft actuators," *Robotics Reports*, vol. 1, no. 1, pp. 31–41, 2023.

[24] M. J. Ford, C. P. Ambulo, T. A. Kent, E. J. Markvicka, C. Pan, J. Malen, T. H. Ware, and C. Majidi, "A multifunctional shape-morphing elastomer with liquid metal inclusions," *Proceedings of the National Academy of Sciences*, vol. 116, no. 43, pp. 21 438–21 444, 2019.

[25] S. I. Rich, V. Nambeesan, R. Khan, and C. Majidi, "Tuning the composition of conductive thermoplastics for stiffness switching and electrically activated healing," *Journal of Intelligent Material Systems and Structures*, vol. 30, no. 18-19, pp. 2908–2918, 2019.

[26] N. Kazem, M. D. Bartlett, and C. Majidi, "Extreme toughening of soft materials with liquid metal," *Advanced Materials*, vol. 30, no. 22, p. 1706594, 2018.

[27] R. Tutika, S. H. Zhou, R. E. Napolitano, and M. D. Bartlett, "Mechanical and functional tradeoffs in multiphase liquid metal, solid particle soft composites," *Advanced Functional Materials*, vol. 28, no. 45, p. 1804336, 2018.

[28] M. I. Ralphs, N. Kemme, P. B. Vartak, E. Joseph, S. Tipnis, S. Turnage, K. N. Solanki, R. Y. Wang, and K. Rykaczewski, "In situ alloying of thermally conductive polymer composites by combining liquid and solid metal microadditives," *ACS applied materials & interfaces*, vol. 10, no. 2, pp. 2083–2092, 2018.

[29] M. H. Malakooti, N. Kazem, J. Yan, C. Pan, E. J. Markvicka, K. Matyjaszewski, and C. Majidi, "Liquid metal supercooling for low-temperature thermoelectric wearables," *Advanced Functional Materials*, p. 1906098, 2019.

[30] R. Tutika, S. Kmiec, A. T. Haque, S. W. Martin, and M. D. Bartlett, "Liquid metal–elastomer soft composites with independently controllable and highly tunable droplet size and volume loading," *ACS applied materials & interfaces*, vol. 11, no. 19, pp. 17 873–17 883, 2019.

[31] J. Wang, G. Cai, S. Li, D. Gao, J. Xiong, and P. S. Lee, "Printable superelastic conductors with extreme stretchability and robust cycling endurance enabled by liquid-metal particles," *Advanced Materials*, vol. 30, no. 16, p. 1706157, 2018.

[32] A. Kataruka and S. B. Hutchens, "Pdms polymerized high internal phase emulsions (polyhipes) with closed-cell, aqueous-filled microcavities," *Soft Matter*, vol. 15, no. 47, pp. 9665–9675, 2019.

[33] Y. Han, H. Tetik, and M. H. Malakooti, "3d soft architectures for stretchable thermoelectric wearables with electrical self-healing and damage tolerance," *Advanced Materials*, p. 2407073.

[34] E. J. Krings, H. Zhang, S. Sarin, J. E. Shield, S. Ryu, and E. J. Markvicka, "Lightweight, thermally conductive liquid metal elastomer composite with independently controllable thermal conductivity and density," *Small*, p. 2104762, 2021.

[35] S. Mei, Y. Gao, Z. Deng, and J. Liu, "Thermally conductive and highly electrically resistive grease through homogeneously dispersing liquid metal droplets inside methyl silicone oil," *Journal of Electronic Packaging*, vol. 136, no. 1, p. 011009, 2014.

[36] S. Pak, M. D. Bartlett, and E. J. Markvicka, "Direct ink write 3d printing of fully dense and functionally graded liquid metal elastomer foams," *Advanced Functional Materials*, p. 2410908.

[37] O. Hur, E. J. Markvicka, and M. D. Bartlett, "Anisotropic and heterogeneous thermal conductivity in programmed liquid metal composites through direct ink writing," *Advanced Functional Materials*, p. 2417375, 2024.

[38] J. W. Boley, E. L. White, and R. K. Kramer, "Mechanically sintered gallium–indium nanoparticles," *Adv. Mater.*, vol. 27, no. 14, pp. 2355–2360, 2015.

[39] Y. Lin, C. Cooper, M. Wang, J. J. Adams, J. Genzer, and M. D. Dickey, "Handwritten, soft circuit boards and antennas using liquid metal nanoparticles," *Small*, vol. 11, no. 48, pp. 6397–6403, 2015.

[40] C. J. Thrasher, Z. J. Farrell, N. J. Morris, C. L. Willey, and C. E. Tabor, "Mechanoresponsive polymerized liquid metal networks," *Advanced Materials*, vol. 31, no. 40, p. 1903864, 2019.

[41] S. Liu, M. C. Yuen, E. L. White, J. W. Boley, B. Deng, G. J. Cheng, and R. Kramer-Bottiglio, "Laser sintering of liquid metal nanoparticles for scalable manufacturing of soft and flexible electronics," *ACS applied materials & interfaces*, vol. 10, no. 33, pp. 28 232–28 241, 2018.

[42] A. Haake, R. Tutika, G. M. Schloer, M. D. Bartlett, and E. J. Markvicka, "On-demand programming of liquid metal-composite microstructures through direct ink write 3d printing," *Advanced Materials*, vol. 34, no. 20, p. 2200182, 2022.

[43] R. Ma, C. Guo, Y. Zhou, and J. Liu, "Electromigration induced break-up phenomena in liquid metal printed thin films," *Journal of electronic materials*, vol. 43, pp. 4255–4261, 2014.

[44] D. Stroud, "Calculations of the average driving force for electromigration in liquid-metal alloys," *Phys. Rev. B*, vol. 13, pp. 4221–4226, May 1976.

[45] S. Kumar, P. Kumar, and R. Pratap, "A model for electromigration induced flow in liquid metals," *Journal of Physics D: Applied Physics*, vol. 50, no. 39, p. 39LT02, Sept. 2017, publisher: IOP Publishing.

[46] I. Dutta and P. Kumar, "Electric current induced liquid metal flow: Application to coating of micropatterned structures," *Applied Physics Letters*, vol. 94, no. 18, p. 184104, may 2009.

[47] R. Sorbello, "Electromigration in liquid metal alloys," *physica status solidi (b)*, vol. 86, no. 2, pp. 671–678, 1978.

[48] H. O. Michaud and S. P. Lacour, "Liquid electromigration in gallium-based biphasic thin films," *APL Materials*, vol. 7, no. 3, mar 2019.

[49] K. L. Dorsey and N. Lazarus, "Lifetime of Liquid Metal Wires for Stretchable Devices," *Advanced Materials Technologies*, vol. n/a, no. n/a, p. 2001100, feb 2021.

[50] N. Grassie and I. Macfarlane, "The thermal degradation of polysiloxanes—i. poly (dimethylsiloxane)," *European polymer journal*, vol. 14, no. 11, pp. 875–884, 1978.

[51] T. A. Pozarycki, D. Hwang, E. J. Barron III, B. T. Wilcox, R. Tutika, and M. D. Bartlett, "Tough bonding of liquid metal-elastomer composites for multifunctional adhesives," *Small*, vol. 18, no. 41, p. 2203700, 2022.

[52] J. M. Taylor, K. Perez-Toralla, R. Aispuro, and S. A. Morin, "Covalent bonding of thermoplastics to rubbers for printable, reel-to-reel

processing in soft robotics and microfluidics," *Advanced Materials*, vol. 30, no. 7, p. 1705333, 2018.